Egyptian Geophysical Society
EGS Journal, Vol. 9, No. 1, 145-153 (2011)

EVALUATION OF THE STRUCTURAL ELEMENTS USING GRAVITY AND MAGNETIC DATA AT SOUTHERN PART OF SINAI PENINSULA, EGYPT

A. Khalil, M.El Bohoty and E. Aboud
National Research Institute of Astronomy and Geophysics, Helwan, Egypt.

تقييم العناصر التركيبية باستخدام بيانات الجاذبية والمغناطيسية الأرضية
فى الجزء الجنوبى من شبه جزيرة سيناء ، مصر

الخلاصة: الهدف من هذه الدراسة هو تقديم دراسة استطلاعية لتوضيح وتحديد التراكيب التحتسطحية في الجزء الجنوبي من شبه جزيرة سيناء باستخدام البيانات الجيوفيزيائية المتاحة والتى تشمل بيانات التثاقلية الأرضية وكذلك خريطة المغناطيسية الأرضية التى تم قياسها من الجو. وقد تم إختيار منطقة الدراسة هذه بسبب وضعها التكتونى النشط. في هذه الدراسة تم تطبيق بعض التقنيات التفسيرية مثل تحويل البيانات المغناطيسية الأرضية إلى القطب الشمالى للأرض وكذلك إستخدام تقنية المرشحات المنخفضة و العالية و النمذجة إلى الأمام فى إجراء عملية الفصل وذلك لمعالجة البيانات المغناطيسية الأرضية و التثاقلية الأرضية بالإضافة إلى إستخدام طريقة ترشيح العدد الموجى وتقنية ميل الظل الشمسى فى محاولة لإظهار أفضل الأوضاع للميل الشمسى. وقد طبقت على ثلاثة أنواع من الترشيحات المختلفة للطول الموجى، كذلك تم تنفيذ التفسير الكمي باستخدام اثنين من النماذج ثنائية الأبعاد والاشارة التحليلية وذلك لتمييز المصادر المتغيرة لأعماق محددة لحالات الشاذات المحلية والإقليمية. وقد تم تشييد ثلاثة قطاعات بواسطة طريقة النمذجة ثنائية الأبعاد. ولتوضيح النطاقات التكتونية و التركيبية فى منطقة الدراسة تم تطبيق طريقتى الطول الموجى و النمذجة ثنائية الأبعاد. ، وقد تم تحديد عمق صخور القاعدة وكذلك تضاريس سطح القاعدة. ومن خلال تحليل النماذج المختلفة وجد أن الفوالق الرئيسية في منطقة الدراسة تتجة غالبا فى اتجاهات شمال غرب– جنوب شرق – وشمال شرق– جنوب غرب و كذلك شرق غرب ووجد أن قيم متوسط عمق صخور القاعدة يتراوح من 0.5 إلى 4 كم وتدخلات القاعدة تتراوح من ٣٥م إلى ٥٠٠ متر

ABSTRACT: *In this study, we present a reconnaissance study to elucidate and delineate the subsurface structures and tectonics of the southern part of the Sinai Peninsula using available geophysical data; including high resolution Bouguer gravity and aeromagnetic data. The study area is selected due to its active tectonic situation. The analysis techniques used are reduction to the pole (RTP), low and high pass filtering and forward modeling to process the aeromagnetic and gravity data. Moreover, wave number filtering and sun shading techniques have been carried out utilizing three types of filters with varying wavelengths. The quantitative interpretation is performed using two dimensional modeling and analytical signal techniques to discriminate the variable sources of specific depth ranges for the residual and regional anomalies. Three basement cross sections have been generated using the 2D-modeling to support and refine the interpreted structures. To reveal the tectonic zones and structures, depth estimations have been conducted by applying the analytical signal and 2D-modeling techniques. It is found that the main tectonics in the study area have NW-SE, NE-SW and E-W trends. It is found that the average depth values to the basement complex range between 0.5 to 4 km and to the basement intrusions 35 m and 500 m.*

INTRODUCTION

The study area lies at the southern part of the Sinai Peninsula between latitudes 27° 30' and 28° 25' north and longitudes 33° 30' and 34° 30' east adjacent to the Gulf of Suez (Fig. 1). The Sinai Peninsula is one of the main geographic units of Egypt and represents the Asiatic part of Egypt. It covers an area of some 61000 km^2. It is triangular in shape, separated geographically from the Eastern Desert by the Gulf of Suez (Fig. 1). Its southern part is considered as unstable shelf due to the frequent earthquake activities and its relation to the tectonic activity of the Red sea, Gulf of Suez and Gulf of Aqaba. The study area is located in the southern part of Sinai Peninsula (Fig. 1).

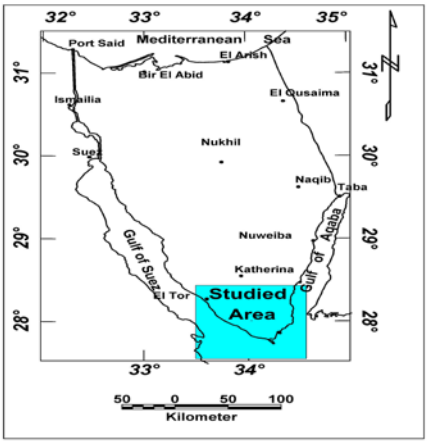

Fig. (1): Location map of the study area.

It is bounded from the east by the south Sinai massive block and from the west by the Gulf of Suez. This work evaluates the subsurface geologic active structures using different processing techniques separating the different sources of magnetic and gravity data.

The potential field data include the following:-

- Gravity data in the form of Bouguer anomaly map compiled by the Egyptian General Petroleum Cooperation (EGPC, 1980).
- Magnetic data in the form of total intensity aeromagnetic anomaly map compiled by the Egyptian General Petroleum Cooperation (1990). The RTP technique is applied to the total aeromagnetic intensity map using the Geosoft program (1998). The input parameters are: inclination 41°, declination 2.4° and a total field strength of 42.350nT. Qualitative interpretation deals with description of anomalies especially their symmetry, strike, extensions, amplitude, gradients, filtering technique and trend analysis. The quantitative interpretation in this work is based on the following steps, for both gravity and magnetic data:

a- Application of regional-residual separation technique on the potential field data.
b- Application of Wave-number and Sun-shading techniques in order to enhance the direction of features of the RTP magnetic data.
c- Application of Up-to date methods for depth estimation.
d- Two-dimensional modeling technique has been applied along some selected magnetic profiles in order to achieve high accuracy for the subsurface basement configuration and the dissected structures.

GEOLOGICAL SETTING

The Sinai Peninsula is the most fascinating region from the geological point of view because it displays a variety of simple and complex structural forms (Abu Al-Izz, 1971). In general, Sinai reflects in miniature all geologic column of Egypt. It is covering an area of some 61000 Km^2, with a triangular shape and is separated geographically from the Eastern Desert by the Gulf of Suez. All features characterizing Egypt's geologic history are found in Sinai. It was subjected to several advances of the paleo-Tethys. Sea water covered it in the north and northwest during the Pre-Cambrian. In Cretaceous and Eocene times, the regression of the sea was complete. Figure (2) shows the main surface geologic units at southern part of Sinai.

For instance, the Paleozoic rocks overly the Precambrian basement in the southwestern part (Omara, 1972; Kora, 1995).

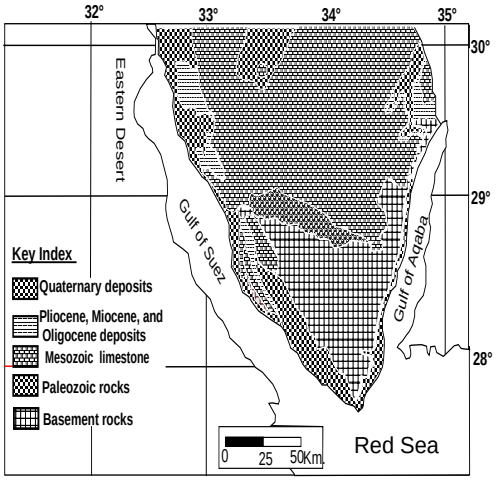

Fig. (2): The main surface geologic units at southern part of Sinai (after Geological Survey of Egypt, (1993).

The Mesozoic strata crop out in northern Sinai where an almost complete sequence from Triassic to Cretaceous is known (Kerdany and Cherif, 1990), while it composes a subsurface section attaining a huge thickness (955 m for Jurassic only) at Ayun Musa. The area under study is a part of the eastern flank of the Gulf of Suez rift and it had been subjected to intensive faulting during the rift activities. There are two main fault structures, the first one runs along the contact between the sedimentary section and the basement complex, while the second one runs along the Gulf of Suez coast to the west. These two main faults are dissected comparatively by minor transversal faults and sometimes they branch to a series of small and roughly parallel step faults. From the geological point of view, the study area is bounded to the east by the igneous and metamorphic rocks of south Sinai Mountains and to the west by Gebel Hammam Sayidna Mussa. The plain is covered by Quaternary deposits and the Upper Tertiary deposits share in the surface geology of El-Qaa plain **(**Abdallah and Abu Khadrah, 1976). To the west of the plain, Eocene limestone and Miocene limestone and Gypsum crop out in succession to form the Gebel Qabeliat Ridge (Said, 1962). El-Shazly et al. (1974) classified the Quaternary sediments into twelve units. Three of these units; the gravel plain, alluvial and wadi deposits are identified in the southern part of the area. The alluvial deposits are very steep near the foothills and gentle near the coast. These deposits are composed mainly of coarse grain sand and granitic boulders with various sizes. The Quaternary deposits become compacted and gradually fine grained towards the central part of Wadi Isla and are composed of cross-bedded sandstone with some gravels.

DATA ANALYSIS AND INTERPRETATION

Integrated geophysical methods (gravity and magnetic) have been applied to determine the subsurface structural and tectonic setting of the study area.

1- Gravity Data

The inspection of the Bouguer anomaly map of the study area (Fig. 3) reveals that the gravity field in the area under study has a maximum relief of about +42 mGal in the southern and central parts, and has a minimum of about - 72 mGal in the northeastern part of the study area. In the central part of the area, the anomaly is considered the strongest positive anomaly as a whole. Such gravity anomalies are suggested to be associated with denser source rocks of basic nature.

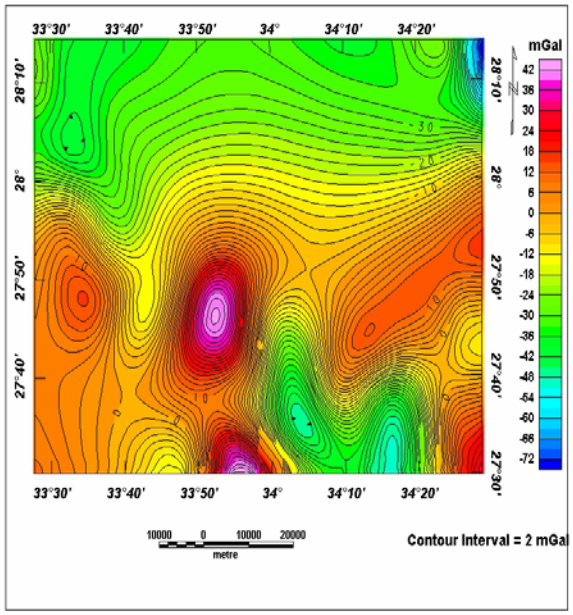

Fig. (3): Bouguer gravity anomaly map of the study area.

The regional gravity field in the central part influences the well-defined local gravity anomalies in the north eastern and south western parts of the area due to lithologic variations either within the basement or in the sedimentary section itself or in both. The general trends of the field are NW-SE and NE-SW. Also, most of the steep gradients have alternating negative and positive anomalies at the north eastern and south western parts of the map, respectively. This indicates that the area is structurally controlled by tectonics having major axis in the NW-SE and NE-SW directions. The south eastern part has anomalies with definite polarities and is characterized by irregular contouring pattern, with negative value, different sizes and shapes and from moderate to high gradients, while the central part has positive value with different sizes and shapes and high gradients. The source of the anomaly may be due to an uplifted block of the denser crystalline rocks.

Gravity Separation

High and low pass filter techniques have been used for filtering the regional and local components using wavenumber 0.01667 km^{-1} using Geosoft programs (Oasis Montaj, 1998). The low pass filter regional map (Fig. 4) shows E-W gradient occupying the central part of the study area and the high gravity anomalies occupying the central part of about 42 mGal. The southeastern and northern parts reflect low gravity anomalies of about -46 mGal. The high pass filter residual map (Fig. 5) reveals high frequency for the gravity anomalies at the southern part while the northern part reveals high gravity anomalies ranging from -2 mGal to 16 mGal. The high pass filter map (residual) suggests that the study area may be dissected by faults trending N-S, NW-SE and NE-SW (Fig. 6). The residual gravity data were used for quantitative gravity interpretation to estimate the depth of the basement complex using the Euler deconvolution technique.

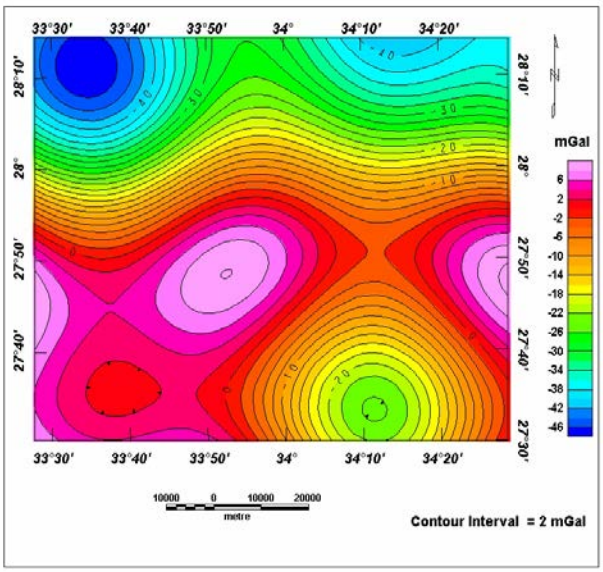

Fig. (4): Regional Bouguer anomaly map (low pass filter) using wavenumber 0.01667 km-1.

3-D Gravity Interpretation (Euler Deconvolution)

3-D gravity interpretation has been applied using the Euler deconvolution technique through GRIDEPTH program which is a part of the Geosoft programs package. Residual gravity data have been used to determine the depth to the tops of the geologic sources (the basaltic sheet) responsible for the observed anomalies. The method used on the program is based in the Euler's homogeneity equation.

The later relates the gravity and magnetic fields and their gradient components to the locations of the sources, with the degree of homogeneity N, which may be interpreted as a structural index (Thompson, 1982). The structural index is a measure of the rate of change of the field with distance. For example, the gravity field of a narrow 2-D dyke, sill, ribbon or step have a structural index of N=0, while a vertical pipe (or cylinder) have N=1. The authors estimate the depths to the gravity sources in the study area using a window size of 10 and structural index of zero. The results are presented in figure 7 which indicates that the study area reflects depth to the basement ranging from 500 to 4000 m.

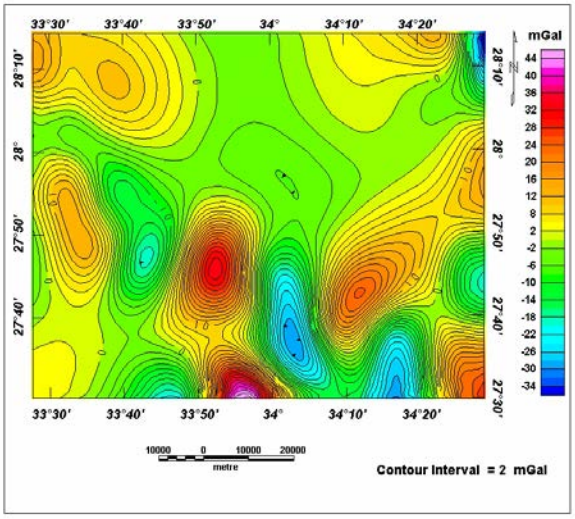

Fig. (5): Residual Bouguer anomaly map (high pass filter): using wavenumber 0.01667Km-1.

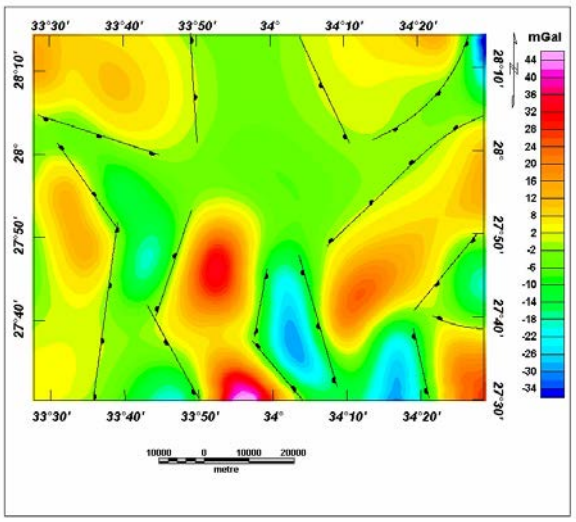

Fig. (6): Fault elements dissect the study area.

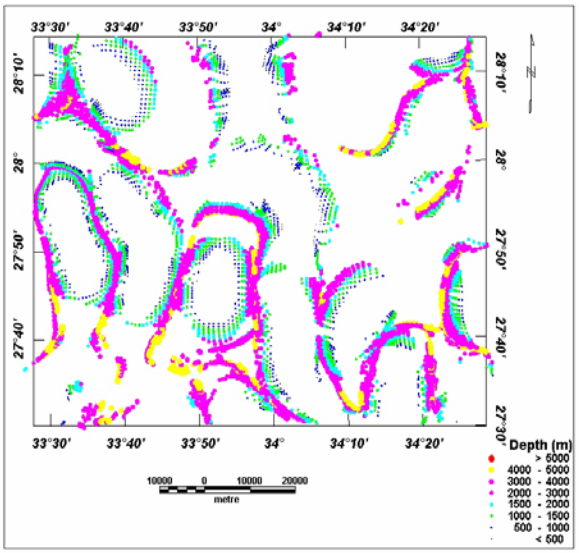

Fig. (7): Euler solutions at different depths.

These results were used to construct a basement relief map (Fig. 8) which indicates that the area reveals deeper depth at the eastern and western parts ranging from 2400 to 4000 m while the northern part is represented by shallow basement depth ranging from 800 to 2200 m.

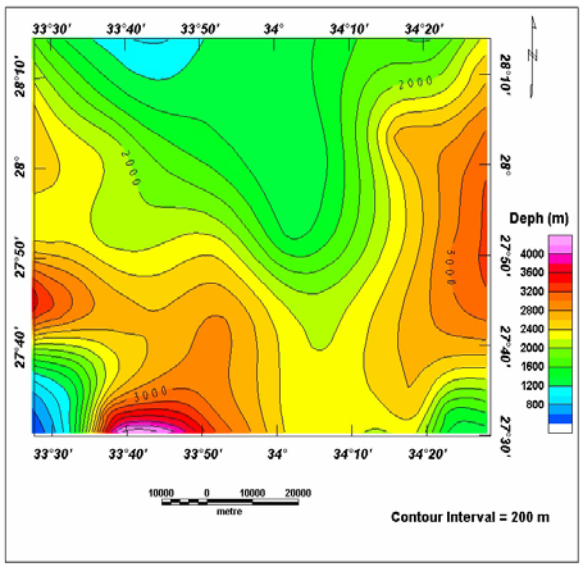

Fig. (8): Basement relief map of the study area.

2- Aeromagnetic Data RTP aeromagnetic map

Aeromagnetic data provide information on both structure and composition of the magnetic basement. It is known that geomagnetic field and the magnetization direction of magnetic body are in general not vertical. As a result, magnetic anomalies are typically shifted laterally from the causative body. This usually complicates the interpretation of magnetic anomalies. One way to simplify the shapes of magnetic anomalies, and to translate anomalies so that they are centered directly above the causative body, is to apply reduction-to- the- pole. Therefore, the aeromagnetic data have been reduced to pole (RTP) using a Geosoft program (1998) with magnetic inclination of 41°, declination 2.4° and a total field strength of 42.350nT. Inspection of the RTP aeromagnetic anomaly map (Fig. 9) indicates that there is a predominance of low magnetic anomalies in the eastern and western parts. The central part is characterized by intense high magnetic anomalies constituting several peaks. These peaks reflect very high magnetic susceptibility with varied amplitudes. These anomalies may be attributed to the occurrence of subsurface basic intrusions of high magnetic content at different depths. Also the differences in magnetic relief between each two adjacent magnetic highs and lows suggest a comparable variation in lithology.

The map also shows local magnetic anomalies superimposed on the regional magnetic field. These anomalies are most probably related to basement faulting structure. Several intensive contour zones indicate high horizontal magnetic gradients and, could

be interpreted as locations of fault planes. Faults trees and axes as magnetic anomalies have N-S trend. Also, the RTP aeromagnetic map (Fig. 9) indicates that most of the magnetic anomalies align themselves in NW-SE, NE-SW, E-W and N-S directions. This may be due tectonics related to the Mediterranean Sea, Gulf of Suez, and Gulf of Aqaba.

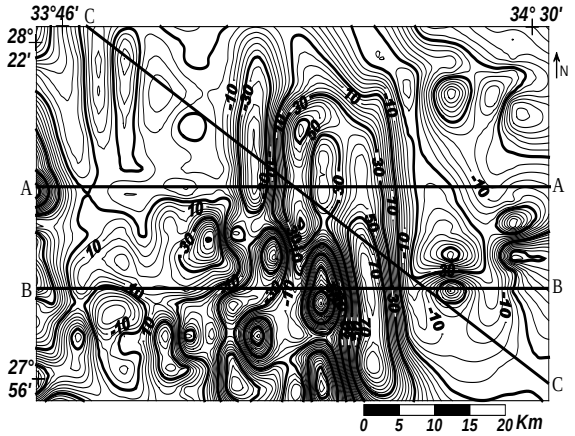

Fig. (9): Total magnetic anomaly map reduced to the pole for the study area (after Egyptian General Petroleum Cooperation (EGPC, 1990) showing the location two-dimensional modeling profiles (A-A, B-B, C-C).

The deepest parts are present in the central and southern parts of the map indicated by presence of negative anomalies. Moreover, it seems that the Gulf of Suez consists of faulted blocks whereas some parts show deepest structure represented by negative values in the southern part of the Gulf. The shallowest parts are extending along the two gulfs and southern part of Sinai where the basement rocks crop out.

Regional-residual separation of the RTP aeromagnetic map

The separation procedures are designed to get a good resolution of the effect of the broad deeper variations "i.e. regional" from that of the sharper local ones "i.e. residual" magnetic components as two distinct magnetic maps. The residual map focuses attention on weaker features, which are obscured by strong regional effects in the original map. The separation of regional magnetic field from the residual one is achieved by applying the least square polynomials approach on the reduced to the pole aeromagnetic data through using the technique of Agrawal and Sivaji (1992). In order to isolate the shallower residual component, the residual map of the fourth order (Fig. 10) is considered as the most suitable and applicable for the magnetic anomalies interpretation.

This map exhibits distinct locations of high magnetic anomalies with high amplitudes and steep gradients located at the central part of the map. In the eastern part of the area, the most striking anomalies is the N-S magnetic low of steep gradient and low frequency. The main low is separated from the high anomalies in the central part by steep magnetic gradients. These magnetic features reflect the thin sedimentary sequence and shallow depth of the basement. The magnetic anomalies across western part are characterized by different polarities (positive and negative) with N-S and E-W trends. The main high anomalies are separated from the low one by steep magnetic gradient.

Filtering

For the purpose of detailed qualitative interpretation of the magnetic anomalies, wavelength filtering has been applied. The term filter refers to systems with frequency-selective frequency responses. These filters allow certain regions of the spectrum to remain undisturbed while other spectral regions are attenuated. Filters are specified by their frequency domain magnitude characteristics. The objective of frequency domain filtering presents a result in a way that makes the data easier to understand and interpret.

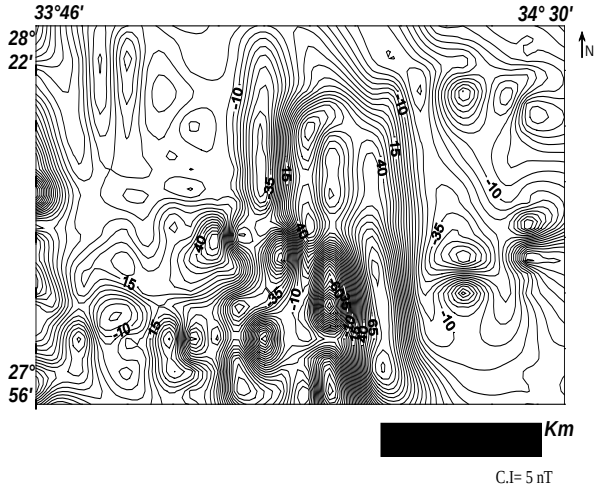

Fig. (10): Residual magnetic anomaly map of the fourth order.

Analysis of Magnetic Filtered Maps

a- Wavenumber filtering technique

One of the main objectives of the wavelength filtering was to attempt to relate the two main regional negative and positive anomalies to their depth of origin, and to identify persistent trends at various wavelength of cut-off. The effective cutoff wavelengths have been selected such that the depths of the mass centers of the causative bodies are in accordance with the results of 2-D gravity modeling; several layers could be defined. Frequency filtering represents a major component of magnetic data processing. As a rule, digital filters are used for signal enhancement that is to remove unwanted noises, and enhance the desired signals. The nature of "noises" and "signals" varies from case to case or even from a stage of processing to another according to its target. In this study, we apply the 2D filtering to the RTP aeromagnetic map to the lineation caused by

faulting or dislocations in the basement rocks at different depths.

In the present work, the wavelength linear filtering of the RTP magnetic data was carried out utilizing three types of filtering; namely the high pass, low pass, and band bass filters. The filtering technique is performed using the cut-off frequency ranging between 0.080 cycle/ unit data and 2.00 cycle/ unit data. The high pass filtered map (Fig 11) elucidates high frequency and short wavelength spot like magnetic anomalies which are inferred as residual component located in the central and southern parts of the study area.

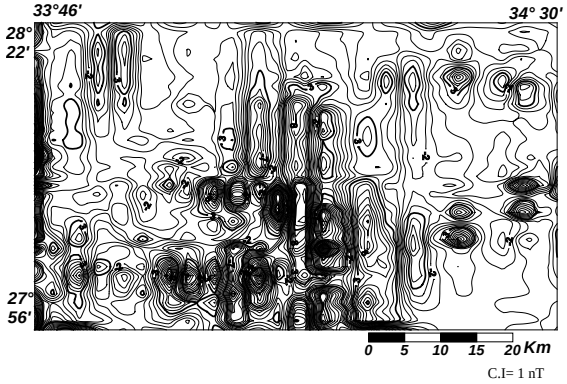

Fig. (11): Moving average high-pass filtered map of the RTP magnetic data.

The prominent NW-SE and NE-SW anomalies in the eastern and western sides of the RTP aeromagnetic map (Fig 9) are found to be distributed with N-S trend in the high pass filter map (Fig. 11). This indicates that the NW-SE and NE-SW trends are confined to the deep part of the area, whereas, the N-S one is dominated in the shallow part. The low pass filtered anomaly map (Fig. 12) shows that the well defined trends of anomalies in the RTP aeromagnetic map (NW-SE and NE-SW) still persist. This reflects the deep extent of the structures causing the anomalies. The band-pass filter (Fig. 13) infers that the dominant trends of anomalies in the original RTP aeromagnetic map still persist. However, some smooth regional anomalies that appear away from any subsurface structure are most probably the result of regional variation in the magnetization or magnetic susceptibility of the rock at moderate depths.

b- Sun-shading filtering

This technique is employed to enhance the directional features of the RTP magnetic data in order to evaluate them as if they form a 3-D topographic surface (Pelton**,** 1987; Cooper, 1997). Therefore, three sun directions are introduced for this operation (45°, 135° and 225°) under the same sun elevation. Moreover, the resulted data are contoured and inspected for each direction.

The RTP map sun-shaded obtained from the sun direction of 45° clockwise from the north and elevation of 20m from the horizontal (Fig. 14) elucidates the shapes and positions of the analyzed positive and negative anomalies at the first 3D topographic representation through the sun direction 45°. This filter tends to exaggerate the anomalies shapes and trends lying normal to the chosen sun azimuth and reduced the parallel ones. Therefore, the trends and anomalies alignments that are discovered in the data set by the use of such filter must trend NW-SE and N-S (i.e. normal to the sun azimuth). Generally, the filter at this azimuth is considered, as if these anomalies have been regarded in the northeastern corner of the map.

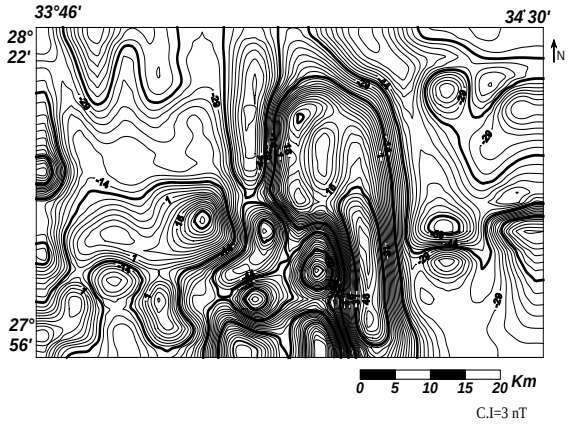

Fig. (12): Moving average low-pass filtered map of the RTP magnetic data.

Fig. (13): Moving average band-pass filtered map of the RTP magnetic data.

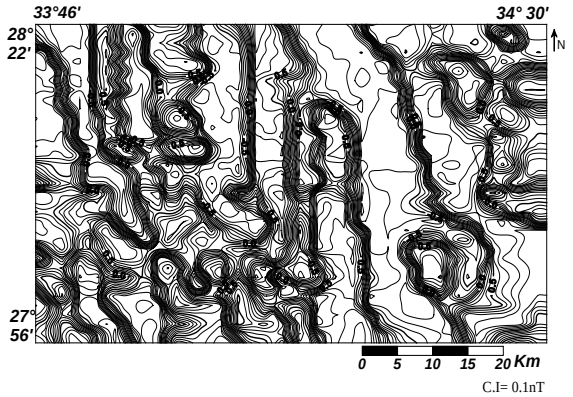

Fig. (14): RTP magnetic map sun-shaded from the sun direction of 45° clockwise from the north and elevation of 20m from the horizontal.

Moreover, by increasing the sun direction to 135° clockwise at the same elevation, the RTP map sun – shaded from the sun direction of 135° clockwise from the north and elevation of 20m from the horizontal (Fig. 15) implies the highest analogy in the configurations and positions of the resulted anomalies are related to the foregoing map in the central part, which are distributed with N-S trend, and the reduction of some anomalies, which are parallel to the shadow direction, i.e. for example the prominent NW-SE anomalies trend in the northeastern side of the map sun shaded from the sun direction of 45° are found to be distributed with NE-SW trend. By increasing the effective shadows on the map data, the RTP map sun-shaded from the sun direction of 225° of clockwise from the north and elevation of 20m from the horizontal (Fig. 16) reflects the shapes and degree of the anomalies lateral extensions, which are illustrated in the map sun- shaded from the sun direction of 45° especially in the eastern and central parts of the map (Fig. 14). The resulted anomalies therefore trend N-S and NW-SE normal to the sun azimuth and the features parallel are reduced.

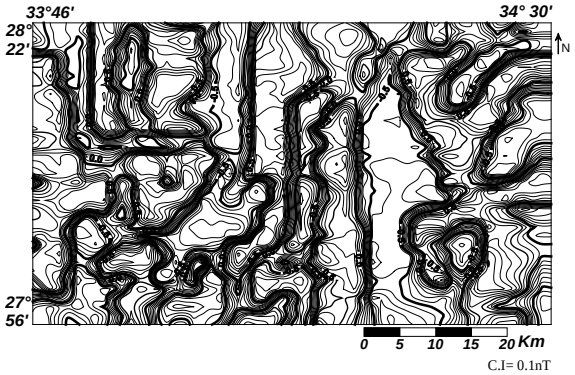

Fig. (15): RTP magnetic map sun-shaded from the sun direction of 135° clockwise from the north and elevation of 20m from the horizontal.

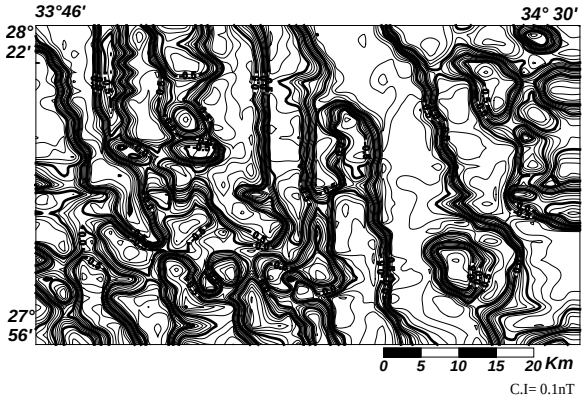

Fig. (16): RTP magnetic map sun-shaded from the sun direction of 255° clockwise from the north and elevation of 20m from the horizontal.

Depth Estimation

The depth to the source of magnetic anomalies is valuable and important in any geophysical interpretation of subsurface structures. Calculation of the depth to the top of the source or the depth to the bottom of the source can be made from the shape of the anomalies or the shape of the power spectrum computed from the potential field data.

3-D Analytical Signal Method

The analytical signal map can be directly used to yield the corresponding depths of the expected source bodies with respect to the level of observation. Figure 17 depicts the analytical signal map of the study area. This map reveals mostly a number of elongated high anomalies trending N-S, which are characterized by increasing the small undulations in their contour lines. These anomalies are separated by a lot of local elements of high relief, small extensions and elongated shapes. Further, this analytical signal map could be directly used to yield the corresponding value for the expected source bodies with respect to the level of observations. The calculated depth values of the buried source bodies range between 1.4 and 1.7 km.

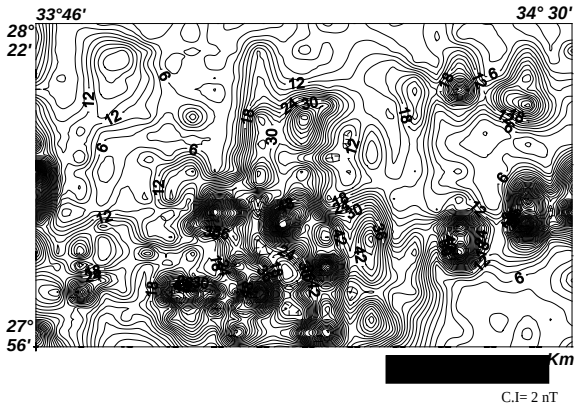

Fig. (17): 3-D analytical signal of RTP aeromagnetic map of the study area.

Two-Dimensional Magnetic Modeling

The two-dimensional modeling usually involves the fitting of geophysical parameters to potential data. Strictly speaking, potential modeling could be an inverse solution to potential problems, which can not be unambiguous. The magnetic modeling involves four separate parameters, top surface, bottom surface, magnetic susceptibility contrast, and the observed magnetic anomaly. If three of these parameters are known or assumed, the fourth may be calculated. The forward modeling specifies the first three items and calculates the anomaly. To confirm the interpreted magnetic basement structural framework of the study area, three regional magnetic profiles have been modeled using the 2D-forward modeling technique. The selected profiles are taken from RTP aeromagnetic map and denoted as A- A, B- B, and C-C (Fig. 9). The magnetic susceptibility contrast values for the different

polygons along the three structural cross-sections have been assumed. The magnetic field is calculated iteratively for these geological models, until a best fit is reached between the observed and calculated curves. The three modeled profiles are shown on Figs (18, 19 and 20). On these three figures, the observed RTP aeromagnetic profile is shown as dashed circular points on the upper half of the figure. The horizontal x-axis represents the horizontal distance in km along the profiles, while the vertical axis is the magnetic field scale, in nano tesla and the lower part represents the depth scale in km. Close examination of these three profiles (Figs. 18, 19 and 20) shows very good fit between the observed and calculated magnetic anomalies. The magnetic susceptibility of the basement rocks is 0.0045 S.I. units. The magnetic field responses computed for the geological models used magnetic declination of 2.4º and magnetic field inclination 41º. The utilized regional magnetic field intensity is 42.350 nT. It is evident from the magnetic modelling along profile A-A (Fig 18) that, the western part is deeper in nature than the central counter part. It is noticed that, the model exhibits two peaks which express the shallowest basement surface.

Fig. (18): 2-D magnetic anomaly modeling along profile A-A.

The depths to the basement surface across those peaks are 750 m and 780 m. It is obviously clear that the depth to the basement increases from the east to the west of the profile. The basement depth is 1.60 km in the western part of the model, while at the eastern part of the profile is about 1.10 km with a general dipping toward the west and uplifting toward the eastern part of the profile. The magnetic susceptibility is 0.0417c.g.s unit. A study of the model along profile B-B (Fig. 19) shows the existence of basement at a depth ranging from 1.00 km to 1.20 km on its eastern and western sides. The model includes local basin of depression in the central part. The depth to the basement across this depression is about 1. 85 km and the magnetic susceptibility is 0.0486 cgs unit.

Fig. (19): 2-D magnetic anomaly modeling along profile B-B.

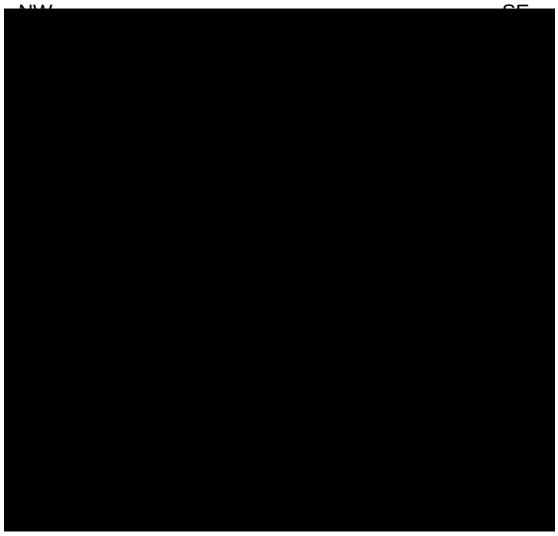

Fig. (20): 2-D magnetic anomaly modeling along profile C-C.

From the investigation of the 2D-model along profile (c-c) which is directed NW-SE and lies in the central part of the area under study, the basement is uplifted in the central part of the profile with a depth of 800 m and dips toward the east and west till reaches 1500 m. The magnetic susceptibility along this profile is 0.0368 cgs unit (Fig. 20).

CONCLUSIONS

Our interpreted gravity and magnetic anomalies of the southern part of Sinai have revealed new information and improved the knowledge about the internal structure beneath this area. The Bouguer anomaly map of the study area reveals that the gravity

field in the area under study has a maximum relief of about +42 mGal in the southern and central parts, and a minimum of about -72 mGal in the northeastern part. The high pass filter map (residual) suggests that the study area could be dissected by different faults trending N-S, NW-SE and NE-SW. 3-D gravity interpretation has been applied using Euler deconvolution technique. The results show that the study area reflects depth to the basement ranging from 500 to 4000 m. The results obtained from the basement relief map indicate that the area reveals deeper depth at the eastern and western parts ranging from 2400 to 4000 m while the northern part is represented by shallow basement depth ranging from 800 to 2200 m. Close examination of the different anomalies through the RTP magnetic maps revealed that the study area is characterized by intensive positive magnetic anomalies with different amplitudes. These anomalies may be attributed to the occurrence of subsurface basic intrusions of high magnetic content at different depths. Also the elongated anomaly zones in the northern part with steep gradients indicate the occurrence of subsurface faulting trending NE-SW. The available magnetic maps of the study area have been separated into their regional and residual anomalies, then a frequency filtering technique has been carried out to isolate the regional (deep-seated structures), the intermediate (intermediate-seated structures) and local (shallow-seated structures) features in order to define better the anomaly configuration, trends and other elements that are difficult to be detected from the original maps. Thus, the considered area is subdivided into three parts, central high anomalies of large sizes and negative polarities in both eastern and western parts. The prominent NW-SE and NE-SW anomalies in the eastern and western sides of the RTP aeromagnetic map are found to be aligned with N-S trend in the high pass filtered map. This indicates that, the NW-SE and NE-SW trends are confined to the deeper part of the area, whereas, the N-S dominates in the shallow part. The band-pass filtered map shows also that, the dominant trends of anomalies in the original RTP aeromagnetic map still persist. However, some smoothed regional anomalies that appear away from any subsurface structures are most probably resulted from the regional variation in the magnetization or magnetic susceptibility of the rocks at moderate depths. It could be noticed that the depths estimated by various determination techniques are in a fairly good agreement; meanwhile, the differences refer to the variations in the basic concepts among these methods. The calculated average depth values indicate that, the average depth to the top of the basement complex range between 0.5 and 4 km while the depth to the basement intrusions ranges between 35m and 0.5 km. Three regional magnetic profiles have been modeled using the 2D-forward modeling technique. Close examination of these profiles shows an excellent fit between the observed and calculated anomalies. They reveal that, the basement rocks in the study area reflect greatly in their composition the assumed wide range of magnetic susceptibility contrast values.

REFERENCES

Abdallah, A.M. and Abu Khadrah, A.M., (1976): Remarks on the geomorphology of the Sinai Peninsula and its associated rocks, Egypt. Geological Survey of Egypt.

Abu Al-Izz, M.S. (1971): Landforms of Egypt. 281p. Dar-A1-Maaref, Cairo, Egypt.

Agrawal, B.N.P. and Sivaji, C.H., (1992): Separation of regional and residual anomalies by least - squares orthogonal polynomial and relaxation by techniques. A performance Evaluation Geophysical Prospection, 40,143-151.

Cooper, G.R.J., (1997): GravMap and PF proc software for filtering geophysical map data. Computers and Geosciences, Vol. 23, No.1, pp.91-101.

Egyptian General Petroleum Cooperation (EGPC) (1990): Aeromagnetic map for Sinai Peninsula (scale 1:100 000).

Egyptian Geological Survey and Mining Authority (EGSMA) (1993): Geologic Map Sinai, Egypt (scale 1:100 000).

El-Shazly, E.M., Abd El Hady., M.A., El-Ghawaby, M.A., and El-Kassas, J.A, (1974): Geology of Sinai Peninsula from ERTS-1 satellite images remote sensing. Remote Sensing Research Project, Academy of Scientific Research and Technology, Cairo, Egypt.

General Petroleum Corporation, A.S.R.T., (1980): Bouguer gravity map of Egypt. Scale 1:500,000.

Kerdany, M., and Cherif, O., (1990): Mesozoic. In: Said R., 1990 (ed.): the geology of Egypt. 407-438, Balkema, Rotterdam.

Kora, M., (1995): An introduction to the stratigraphy of Egypt. Lecture notes, Geology Dept. Mansoura Univ., 116pp.

Oasis Montaj, (1998): Geosoft mapping and application system, Inc, Suit 500, Richmond St. West Toronto, On Canada N5SIV6.

Omara, S., (1972): An early Cambrian outcrop in southwestern Sinai, Egypt. N.JP. Geol. Palaeontol. 5, 306-314.

Pelton, C., (1987): A computer program for hill-shading topographic data sets. Computer and Geosciences, 13, No5, p.545-548.

Said, R. (1962): The geology of Egypt, Amsterdam, Elsevier, Pub. Co., 377 p.

Thompson, D.T. (1982): EULDPH – A new technique for making computer-assisted depth estimates from magnetic data, Geophysics, 47, 31-37.